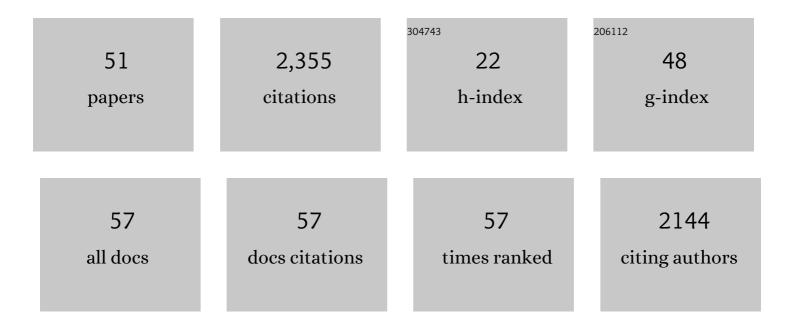
## **Clifford R Bowers**

List of Publications by Year in descending order

Source: https://exaly.com/author-pdf/553028/publications.pdf Version: 2024-02-01



#	Article	IF	CITATIONS
1	Parahydrogen and synthesis allow dramatically enhanced nuclear alignment. Journal of the American Chemical Society, 1987, 109, 5541-5542.	13.7	859
2	Comparison of Structural and Chemical Properties of Black and Red Human Hair Melanosomes¶. Photochemistry and Photobiology, 2005, 81, 135.	2.5	160
3	High capacity production of >65% spin polarized xenon-129 for NMR spectroscopy and imaging. Journal of Magnetic Resonance, 2002, 159, 175-182.	2.1	107
4	Strong Metal–Support Interactions Enhance the Pairwise Selectivity of Parahydrogen Addition over Ir/TiO <sub>2</sub> . ACS Catalysis, 2016, 6, 974-978.	11.2	80
5	Comparisons of the Structural and Chemical Properties of Melanosomes Isolated from Retinal Pigment Epithelium, Iris and Choroid of Newborn and Mature Bovine Eyes¶. Photochemistry and Photobiology, 2005, 81, 510.	2.5	79
6	Silicaâ€Encapsulated Ptâ€&n Intermetallic Nanoparticles: A Robust Catalytic Platform for Parahydrogenâ€Induced Polarization of Gases and Liquids. Angewandte Chemie - International Edition, 2017, 56, 3925-3929.	13.8	73
7	Shaped Ceria Nanocrystals Catalyze Efficient and Selective Paraâ€Hydrogenâ€Enhanced Polarization. Angewandte Chemie - International Edition, 2015, 54, 14270-14275.	13.8	70
8	Solid-state cross-polarization magic angle spinning13C and15N NMR characterization ofSepia melanin,Sepia melanin free acid andHuman hair melanin in comparison with several model compounds. Magnetic Resonance in Chemistry, 2003, 41, 466-474.	1.9	68
9	Observation of a node in the quantum oscillations induced by microwave radiation. Solid State Communications, 2004, 130, 379-381.	1.9	62
10	Parahydrogen-Induced Polarization by Pairwise Replacement Catalysis on Pt and Ir Nanoparticles. Journal of the American Chemical Society, 2015, 137, 1938-1946.	13.7	56
11	Cyclic polyacetylene. Nature Chemistry, 2021, 13, 792-799.	13.6	51
12	Local and Collective Motions in Precise Polyolefins with Alkyl Branches: A Combination of <sup>2</sup> H and <sup>13</sup> C Solid‣tate NMR Spectroscopy. Angewandte Chemie - International Edition, 2009, 48, 4617-4620.	13.8	46
13	Direct Observation of Atoms Entering and Exitingl-Alanyl-I-valine Nanotubes by Hyperpolarized Xenon-129 NMR. Journal of the American Chemical Society, 2007, 129, 13997-14002.	13.7	38
14	Molecular Wheels as Nanoporous Materials: Differing Modes of Gas Diffusion through Ga <sub>10</sub> and Ga <sub>18</sub> Wheels Probed by Hyperpolarized <sup>129</sup> Xe NMR Spectroscopy. Journal of the American Chemical Society, 2010, 132, 5387-5393.	13.7	38
15	Silicaâ€Encapsulated Ptâ€&n Intermetallic Nanoparticles: A Robust Catalytic Platform for Parahydrogenâ€Induced Polarization of Gases and Liquids. Angewandte Chemie, 2017, 129, 3983-3987.	2.0	37
16	Observation of Singleâ€File Diffusion in Dipeptide Nanotubes by Continuousâ€Flow Hyperpolarized Xenonâ€129 NMR Spectroscopy. ChemPhysChem, 2007, 8, 2077-2081.	2.1	35
17	Ultra‣ow Loading Pt/CeO <sub>2</sub> Catalysts: Ceria Facet Effect Affords Improved Pairwise Selectivity for Parahydrogen Enhanced NMR Spectroscopy. Angewandte Chemie - International Edition, 2021, 60, 4038-4042.	13.8	32
18	Surface-Mediated Hyperpolarization of Liquid Water from Parahydrogen. CheM, 2018, 4, 1387-1403.	11.7	31

CLIFFORD R BOWERS

#	Article	IF	CITATIONS
19	Parahydrogen enhanced NMR reveals correlations in selective hydrogenation of triple bonds over supported Pt catalyst. Physical Chemistry Chemical Physics, 2015, 17, 26121-26129.	2.8	29
20	Porosity of Pillared Clays Studied by Hyperpolarized129Xe NMR Spectroscopy and Xe Adsorption Isotherms. Langmuir, 2013, 29, 643-652.	3.5	27
21	Semihydrogenation of Propyne over Cerium Oxide Nanorods, Nanocubes, and Nanoâ€Octahedra: Facetâ€Dependent Parahydrogenâ€Induced Polarization. ChemCatChem, 2016, 8, 2197-2201.	3.7	26
22	Guest Inclusion Modulates Concentration and Persistence of Photogenerated Radicals in Assembled Triphenylamine Macrocycles. Journal of the American Chemical Society, 2020, 142, 502-511.	13.7	23
23	Xenon in <scp>l</scp> -Alanyl- <scp>l</scp> -Valine Nanochannels: A Highly Ideal Molecular Single-File System. Journal of Physical Chemistry Letters, 2013, 4, 3263-3267.	4.6	22
24	Single-crystal-to-single-crystal guest exchange in columnar assembled brominated triphenylamine bis-urea macrocycles. Chemical Communications, 2019, 55, 5619-5622.	4.1	21
25	Comparison of Structural and Chemical Properties of Black and Red Human Hair Melanosomes <sup>¶</sup> . Photochemistry and Photobiology, 2005, 81, 135-144.	2.5	20
26	Crystalline Bis-urea Nanochannel Architectures Tailored for Single-File Diffusion Studies. ACS Nano, 2015, 9, 6343-6353.	14.6	20
27	Single-File Nanochannel Persistence Lengths from NMR. Analytical Chemistry, 2014, 86, 2200-2204.	6.5	17
28	Toward Continuousâ€Flow Hyperpolarisation of Metabolites via Heterogenous Catalysis, Sideâ€Armâ€Hydrogenation, and Membrane Dissolution of Parahydrogen. ChemPhysChem, 2021, 22, 822-827.	2.1	15
29	Cyclopropane Hydrogenation vs Isomerization over Pt and Pt–Sn Intermetallic Nanoparticle Catalysts: A Parahydrogen Spin-Labeling Study. Journal of Physical Chemistry C, 2020, 124, 8304-8309.	3.1	14
30	Implementation of Protocols To Enable Doctoral Training in Physical and Computational Chemistry of a Blind Graduate Student. Journal of Chemical Education, 2015, 92, 1280-1283.	2.3	13
31	An inexpensive apparatus for up to 97% continuous-flow parahydrogen enrichment using liquid helium. Journal of Magnetic Resonance, 2020, 321, 106869.	2.1	13
32	Pairwise semi-hydrogenation of alkyne to <i>cis</i> -alkene on platinum-tin intermetallic compounds. Nanoscale, 2020, 12, 8519-8524.	5.6	12
33	Comparisons of the Structural and Chemical Properties of Melanosomes Isolated from Retinal Pigment Epithelium, Iris and Choroid of Newborn and Mature Bovine Eyes <sup>¶</sup> . Photochemistry and Photobiology, 2005, 81, 510-516.	2.5	11
34	Molecular dynamics in precision deuteriomethyl branched polyethylene from solid-state deuterium NMR. Polymer, 2012, 53, 2633-2642.	3.8	11
35	Persistent Radicals of Selfâ€assembled Benzophenone <i>bis</i> â€Urea Macrocycles: Characterization and Application as a Polarizing Agent for Solidâ€state DNP MAS Spectroscopy. Chemistry - A European Journal, 2017, 23, 8315-8319.	3.3	11
36	Two-dimensional nuclear magnetic resonance spectroscopy in optically pumped semiconductors. Chemical Physics Letters, 2004, 397, 96-100.	2.6	9

#	Article	IF	CITATIONS
37	Single-File Diffusion of Gas Mixtures in Nanochannels of the Dipeptide <scp>l</scp> -Ala- <scp>l</scp> -Val: High-Field Diffusion NMR Study. Journal of Physical Chemistry C, 2016, 120, 9914-9919.	3.1	9
38	Atomic-Scale Structure of Mesoporous Silica-Encapsulated Pt and PtSn Nanoparticles Revealed by Dynamic Nuclear Polarization-Enhanced 29Si MAS NMR Spectroscopy. Journal of Physical Chemistry C, 2019, 123, 7299-7307.	3.1	9
39	Dramatic Enhancement of Hyperpolarized Xenon-129 2D-NMR Exchange Cross-Peak Signals in Nanotubes by Interruption of the Gas Flow. Journal of the American Chemical Society, 2008, 130, 2390-2391.	13.7	8
40	Silica-Encapsulated Intermetallic Nanoparticles for Highly Active and Selective Heterogeneous Catalysis. Accounts of Materials Research, 2021, 2, 1190-1202.	11.7	8
41	Signatures of normal and anomalous diffusion in nanotube systems by NMR. Microporous and Mesoporous Materials, 2013, 178, 119-122.	4.4	7
42	Molecular Motion of the Junction Points in Model Networks Prepared by Acyclic Triene Metathesis. Macromolecular Rapid Communications, 2016, 37, 527-531.	3.9	6
43	Dynamic nuclear polarization and nuclear magnetic resonance in the vicinity of edge states of a 2DES in GaAs quantum wells. Solid State Nuclear Magnetic Resonance, 2006, 29, 52-65.	2.3	5
44	Branch-Induced Heterogeneous Chain Motion in Precision Polyolefins. Macromolecules, 2015, 48, 8858-8866.	4.8	5
45	Ultra‣ow Loading Pt/CeO 2 Catalysts: Ceria Facet Effect Affords Improved Pairwise Selectivity for Parahydrogen Enhanced NMR Spectroscopy. Angewandte Chemie, 2021, 133, 4084-4088.	2.0	5
46	Low-Temperature <sup>23</sup> Na MAS NMR Reveals Dynamic Effects and Compositions for the Large and Small Channels in the Zeolite-Like Ge-Framework of Na <sub>1–<i>x</i></sub> Ge <sub>3+<i>z</i></sub> Materials. Journal of Physical Chemistry C, 2014, 118, 28890-28897.	3.1	4
47	Squeezing xenon into phenylether bis-urea nanochannels. Canadian Journal of Chemistry, 2015, 93, 1031-1034.	1.1	4
48	Mesoporous Silica Encapsulated Platinum–Tin Intermetallic Nanoparticles Catalyze Hydrogenation with an Unprecedented 20% Pairwise Selectivity for Parahydrogen Enhanced Nuclear Magnetic Resonance. Journal of Physical Chemistry Letters, 2022, 13, 4125-4132.	4.6	4
49	Characterization of elastic interactions in GaAs/Si composites by optically pumped nuclear magnetic resonance. Journal of Applied Physics, 2016, 120, 085104.	2.5	2
50	Editorial: The Fourteenth International Bologna Conference on Magnetic Resonance in Porous Media (MRPM14). Magnetic Resonance Imaging, 2019, 56, 1-2.	1.8	1
51	Frontispiece: Shaped Ceria Nanocrystals Catalyze Efficient and Selective Paraâ€Hydrogenâ€Enhanced Polarization. Angewandte Chemie - International Edition, 2015, 54, .	13.8	0